Optical feedback effects on terahertz quantum cascade lasers: modelling and applications

RAKIC, Aleksander D., LIM, Yah Leng, TAIMRE, Thomas, AGNEW, Gary, QI, Xiaoqiong, BERTLING, Karl, HAN, She, KUNDU, Iman, GRIER, Andrew, IKONIC, Zoran, VALAVANIS, Alexander, DEMIC, Aleksandar, KEELEY, James, LI, Lianhe H., LINFIELD, Edmund H., DAVIES, A. Giles, HARRISON, Paul <http://orcid.org/0000-0001-6117-0896>, FERGUSON, Blake, WALKER, Graeme, PROW, Tarl, INDJIN, Dragan and SOYER, H. Peter

Optical feedback effects on terahertz quantum cascade lasers: modelling and applications

Aleksandar D. Rakić,[a*] Yah Leng Lim,[a] Thomas Taimre,[b] Gary Agnew,[a] Xiaoqiong Qi,[a] Karl Bertling,[a] She Han,[a] Stephen J. Wilson,[a] Iman Kundu,[c] Andrew Grier,[c] Zoran Ikonić,[c] Alexander Valavanis,[c] Aleksandar Demić,[c] James Keeley,[c] Lianhe H. Li,[c] Edmund H. Linfield,[c] A. Giles Davies,[c] Paul Harrison,[d] Blake Ferguson,[e] Graeme Walker,[e] Tarl Prow,[f] Dragan Indjin,[c] and H. Peter Soyer[f]

[a]School of Information Technology and Electrical Engineering, The University of Queensland, Brisbane, QLD 4072, Australia;

[b]School of Mathematics and Physics, The University of Queensland, Brisbane, QLD 4072, Australia;

[c]School of Electronic and Electrical Engineering, University of Leeds, Leeds LS2 9JT, United Kingdom;

[d]Materials and Engineering Research Institute, Sheffield Hallam University, Sheffield S1 1WB, United Kingdom;

[e]Cancer Program, Queensland Institute of Medical Research, Herston, QLD 4006, Australia;

[f]Dermatology Research Centre, The University of Queensland, School of Medicine, Translational Research Institute, Brisbane, QLD 4102, Australia

*** rakic@itee.uq.edu.au**

ABSTRACT

Terahertz (THz) quantum cascade lasers (QCLs) are compact sources of radiation in the 1–5 THz range with significant potential for applications in sensing and imaging. Laser feedback interferometry (LFI) with THz QCLs is a technique utilizing the sensitivity of the QCL to the radiation reflected back into the laser cavity from an external target. We will discuss modelling techniques and explore the applications of LFI in biological tissue imaging and will show that the confocal nature of the QCL in LFI systems, with their innate capacity for depth sectioning, makes them suitable for skin diagnostics with the well-known advantages of more conventional confocal microscopes. A demonstration of discrimination of neoplasia from healthy tissue using a THz, LFI-based system in the context of melanoma is presented using a transgenic mouse model.

Keywords: Terahertz imaging; Laser feedback interferometry; Quantum cascade lasers; Tissue imaging.

1. INTRODUCTION

Over the past decade the quantum cascade laser (QCL) has established itself as one of the most promising radiation sources for imaging applications at terahertz (THz) frequencies within the 1–5 THz range. This is largely due to the ability of the THz QCL to generate high-power, coherent, continuous-wave (cw) emission with quantum noise-limited linewidths.[1–8] This makes THz QCLs particularly suited to the development of interferometric THz sensing and imaging systems.[9–11]

Due to the inherently low penetration depth of THz radiation in hydrated biological tissue, biological and particularly superficial skin imaging are applications to which THz frequency imaging is well suited.[17–30] As such, imaging of superficial skin employing THz QCLs in confocal reflection-mode system geometry is an ideal application for the technique.[31, 32] Laser feedback interferometry (LFI) with THz QCLs exploits the interferometric nature of optical feedback in a THz QCL to create a homodyning THz transceiver operating in confocal configuration.[12] This results in a highly sensitive swept-frequency scheme for sensing, imaging, and materials analysis at THz frequencies.[9,13–16] The frequency sweep required to create the LFI signal is commonly generated by modulating the laser current.[9,12]

Infrared, Millimeter-Wave, and Terahertz Technologies IV, edited by Cunlin Zhang, Xi-Cheng Zhang, Masahiko Tani, Proc. of SPIE Vol. 10030, 1003016 · © 2016 SPIE
CCC code: 0277-786X/16/$18 · doi: 10.1117/12.2250621

Most THz LFI systems to date have employed THz QCLs operating in the cw regime at cryogenic temperatures. However, THz QCLs have been demonstrated with peak output powers in pulsed regime exceeding 1 W and operating at temperatures as high as 200 K.[33, 34] Developing technologies and techniques for pulsed THz QCL LFI is therefore an important objective for elevated temperature applications.

In this paper we introduce the concept of pulsed laser LFI whereby the frequency sweep is generated by the transient in laser temperature, not the current modulation. To move towards a realization of pulsed THz LFI,[35] we investigate the behavior of the pulsed THz QCL using reduced rate equation (RRE) models.[36–39] This would enable higher-temperature applications in sensing, imaging, and materials analysis employing LFI using THz QCLs, thereby increasing the applicability of the approach. Moreover, many applications benefit from a wide frequency tuning range.[40, 41] One way to achieve this with THz QCLs is through the use of a coupled-cavity (CC) device.[39, 42–44] It is our view that pulsed operation together with the wide frequency tuning capability of CC THz QCLs will be instrumental in the next generation of LFI at THz frequencies.

We show that both the temperature and the current modulation schemes can be used to create LFI interferograms; we then apply the latter to show the effectiveness of the technique by imaging fresh skin tissue from a transgenic mouse model of malignant melanoma. The Cdk4 R24C/R24C: Tyr- NRAS Q 61K model, in which malignant melanoma can be initiated and promoted by UV exposure, provides skin specimens densely populated with lesions progressing from dermal naevi to invasive cancer extending to deeper tissue. Typically, early stage lesions are not detectable in the visible portion of the electromagnetic spectrum when observed from the epidermis, but are detectable using LFI with a THz QCL.

The remainder of this paper is structured as follows. In Section 2, we briefly review the basic structure and operating principles of LFI. In Section 3, we present a single-mode single-cavity THz QCL RRE model and explore its behavior under pulsed operation. In Section 4, we present calculated results obtained from our RRE model applied to a multi-mode coupled-cavity THz QCL which operates in pulsed mode. In Section 5, we present an LFI experiment which uses the cw current modulation of a THz QCL for imaging melanoma lesions in the transgenic mouse model. Results of the LFI imaging and correlated histology are then shown. Finally, in Section 6, we conclude with a forward-looking discussion.

2. SELF-MIXING PHENOMENON IN THZ QCLS

The self-mixing (SM) phenomenon refers to the perturbation of laser operating parameters by emitted radiation that is retro-injected.[45] This effect is remarkably universal, having been demonstrated at numerous wavelengths and with different device structures, including in THz QCLs.[46–54] The SM effect, while regarded as a nuisance in telecommunications applications, has been harnessed for a range of sensing purposes, including the measurement of displacement, velocity, and fluid flow, as well as for imaging.

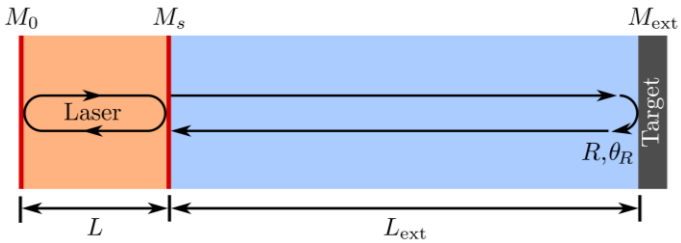

Figure 1. Three mirror model for a laser under feedback. Light recirculates in the laser cavity between mirrors M_0 and M_s — solid arrows in laser cavity of length L. Light exits through M_s, is reflected from the external target M_{ext}, and is reinjected into the laser cavity — solid arrows in external cavity of length L_{ext}.

The basic structure and operating principles of a generic SM interferometer are shown in Fig. 1. The retro-injected light interferes ("mixes") with the intra-cavity electric field, causing perturbations to the laser operating parameters such as the threshold gain, emitted power, lasing spectrum, and laser terminal voltage.[12, 55–58] Whilst this optical feedback affects almost all laser parameters, the two that are most conveniently monitored are the emitted optical power and the voltage across the laser terminals. Of these, monitoring the laser terminal voltage is preferred as it obviates the need for an external THz detector.[13] The small voltage variation (referred to as the "SM signal") depends on both the amplitude and phase of the electric field of the reflected laser beam.

This configuration thus creates a compact, coherent sensor that can probe information about the external target, including its complex reflectivity. The coherent nature of an SM sensor provides very high detection sensitivity, potentially at the quantum noise limit, and therefore a high signal-to-noise ratio can be expected in the SM signal. In the case of THz QCLs, the lifetime of the upper state of the lasing transition is limited by elastic and inelastic scattering mechanisms to a few picoseconds,[59,60] enabling response frequencies of this sensing scheme on the order of tens of GHz.[61–64]

In order to investigate the behavior SM signals from a pulsed THz QCL, we first present a realistic RRE model for a single-mode single-cavity THz QCL under optical feedback. This model permits us to realistically gauge SM signals resulting from thermally-induced frequency modulation.

3. SINGLE-MODE SINGLE-CAVITY THZ QCL RRE MODEL

In this section we use a realistic model[36] of a single-mode, single cavity bound-to-continuum THz QCL, with the aim of illustrating SM signals[65] obtained under low duty cycle pulsed excitation. The rate equations for this model, which include optical feedback and a thermal model,[37] read as follows:

$$\frac{\mathrm{d}S(t)}{\mathrm{d}t} = -\frac{1}{\tau_\mathrm{p}}\,S(t) + M\frac{\beta_\mathrm{sp}}{\tau_\mathrm{sp}(T,V)}\,N_3(t) + MG(T,V)(N_3(t)-N_2(t))\,S(t) + \underbrace{\frac{2\kappa}{\tau_\mathrm{in}}\,(S(t)S(t-\tau_\mathrm{ext}(t)))^{\frac{1}{2}}\,\cos\left(\omega_\mathrm{th}\tau_\mathrm{ext}+\varphi(t)-\varphi(t-\tau_\mathrm{ext})\right)}_{\text{Feedback Term}}, \tag{1}$$

$$\frac{\mathrm{d}\varphi(t)}{\mathrm{d}t} = \frac{\alpha}{2}\left(G(N_3(t)-N_2(t)) - \frac{1}{\tau_\mathrm{p}}\right) - \underbrace{\frac{\kappa}{\tau_\mathrm{in}}\left(\frac{S(t-\tau_\mathrm{ext}(t))}{S(t)}\right)^{\frac{1}{2}}\,\sin\left(\omega_\mathrm{th}\tau_\mathrm{ext}+\varphi(t)-\varphi(t-\tau_\mathrm{ext})\right)}_{\text{Feedback Term}}, \tag{2}$$

$$\frac{\mathrm{d}N_3(t)}{\mathrm{d}t} = -G(T,V)(N_3(t)-N_2(t))\,S(t) - \frac{1}{\tau_3(T,V)}\,N_3(t) + \frac{\eta_3(T,V)}{q}\,I(t), \tag{3}$$

$$\frac{\mathrm{d}N_2(t)}{\mathrm{d}t} = +G(T,V)(N_3(t)-N_2(t))\,S(t) + \left(\frac{1}{\tau_{32}(T,V)} + \frac{1}{\tau_\mathrm{sp}(T,V)}\right)N_3(t) - \frac{1}{\tau_2\ (T,V)}\,N_2(t) + \frac{\eta_2(T,V)}{q}\,I(t), \tag{4}$$

$$\frac{\mathrm{d}T(t)}{\mathrm{d}t} = \frac{1}{mc_\mathrm{p}(T)}\left(I(t)V(T(t),I(t)) - \frac{(T(t)-T_0(t))}{R_\mathrm{th}(T)}\right). \tag{5}$$

In material analysis applications,[9, 16] the magnitude and phase of light reflected by the target material will be altered in a material-dependent manner. This magnitude and phase information can be extracted from the SM signal and used together with reference materials to compute the material's complex reflectivity.

We illustrate the effects of a magnitude and phase shift on the SM signal by simulating an LFI application with thermal modulation.[38] For the purpose of the simulation, the external cavity length was set to L = 2.272 m, the cryostat's cold finger temperature to T_0 = 45 K, and the re-injection loss to ε = 0.005. The excitation current was a rectangular pulse of amplitude 510 mA and duration of 20 μs. Figure 2 shows the results.

Trace (a) in Fig. 2 is the optical output power when no optical feedback is present, for reference. The decay characteristic visible in optical output power is due to increasing temperature caused by self-heating in the active region. When optical feedback is present [trace (b)], LFI fringes are visible in the response. Trace (b) shows optical output power when the reflectivity of the target is 0.7, giving an Acket's characteristic parameter[66, 67] value of C = 1.93, and no phase shift is introduced by the reflection. Self-mixing fringes caused by thermally-induced frequency change can be seen in this trace, with spacing that increases as the temperature and hence frequency change diminishes with time. When the reflectivity of the target is decreased to 0.3, the self-mixing signal [trace(c)] is seen to both diminish in amplitude and to have a slightly different shape. With target reflectivity as before (0.7), and introducing only a phase change of π/3 in the reflected light, the self-mixing fringes [trace (d)] are identical to those of trace (b), but are shifted on the time axis. Real materials would typically produce a combination of both effects, from which the complex reflectivity and hence refractive index may be extracted.

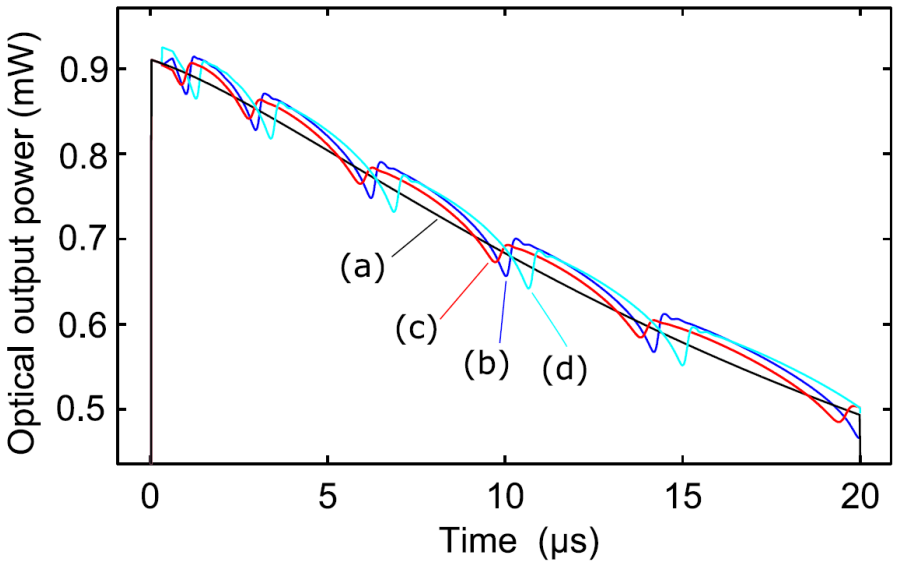

Figure 2. Self-mixing signals generated by LFI with thermal modulation. Trace (a) is a reference trace with no optical feedback present, and shows decay in optical output due to self-heating in the device. Trace (b) shows self-mixing fringes seen when target reflectivity R = 0.7 and trace (c) corresponds to R = 0.3. With reflectivity R = 0.7 and introducing a phase shift of π/3 in the reflected light, trace (d) is obtained.

To complement this single-mode single-cavity RRE model, we now discuss the results of an analogous RRE model for a multi-mode coupled-cavity THz QCL under optical feedback.

4. MULTI-MODE COUPLED-CAVITY THZ QCL RRE MODEL

Coupled-cavity (CC) THz QCLs can provide fast frequency tuning by control of the passive cavity current where localized electrical heating in an optically coupled passive cavity permits selection from and stepping through several discrete lasing modes. A CC THz QCL is composed of two cavities separated by an air gap, the active cavity is electrically driven above the lasing threshold while the passive cavity is operated below threshold to control the dominant mode of the device. Based on the scattering matrix method, the eigenmodes $\omega_{th,m}$ may be calculated by the transmission coefficient of the device. The multi-mode emission power in the presence of optical feedback can be described by multi-mode RREs, which are an extension of those for single-mode QCLs based on a classical three-level QCL model.[68, 69]

Figure 3 shows the simulation output for a CC THz QCL with an active cavity length of 1.5 mm, air gap length of 13 μm, and passive cavity length of 1.582 mm. The passive cavity of the CC THz QCL was driven by a series of current pulses with three different amplitudes of 0 A, 1.4 A, and 2.15 A, all of duration of 20 μs and repetition rate 25 kHz. Near the end of each passive cavity pulse, the active cavity was simultaneously excited with a pulse of duration of 2 μs. Tuning of the passive cavity pulse amplitude results in numerically predicted laser emission at 2.794 THz, 2.766 THz, and 2.738 THz, respectively within the 2 μs during which the active pulse is applied. The amplitude of the active cavity drive current pulses were 510 mA, 520 mA, and 540 mA, respectively considering the threshold current for the emission of three different modes at 2.794 THz, 2.766 THz, and 2.738 THz are 0.46 mA, 0.47 mA, and 0.49 mA. The changes in active cavity lattice temperature induced by the three drive pulses are 4.86 K, 4.94 K, and 5.11 K, respectively. The resulting changes in emission frequency at the three different modes are about 243 MHz, 247 MHz, and 256 MHz, respectively. In the presence of optical feedback these frequency changes result in variations in optical power, indicated by solid lines in Fig. 3, which contain the high frequency component of the SM signal. The SM signals at 2.794 THz (mode 4), 2.766 THz (mode 3), and 2.738 THz (mode 2) are indicated by blue, green and orange lines, respectively. The output power without optical feedback is indicated by broken lines for reference.

The calculations suggest that self-mixing signals at various frequency bands may be obtained by using thermal effects simultaneously in both cavities of CC THz QCLs, enabling THz sensing or imaging over a wider spectral range, therefore unique spectral features of a target under test within multiple frequency ranges can be obtained.

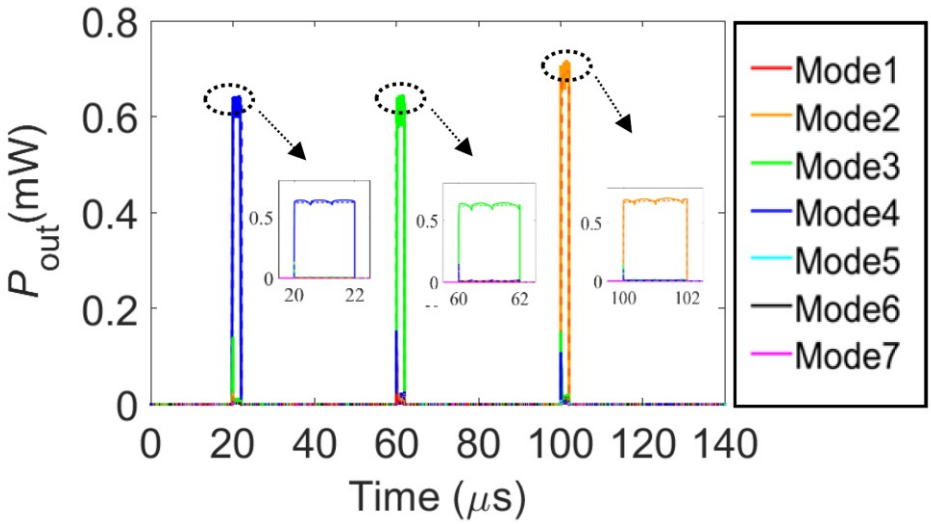

Figure 3. Self-mixing response at three different frequency bands generated by LFI with thermal modulation in a coupled-cavity THz QCL. Blue, green, and orange solid curves indicate the output power at mode 4, 3, and 2, respectively with optical feedback when target reflectivity R = 0.7, and dashed lines indicate the cases without optical feedback.

5. MALIGNANT MELANOMA IMAGING IN MOUSE MODEL

To illustrate the potential of LFI at THz frequencies in biological applications, we now present an experiment which seeks to image malignant melanoma precursor lesions in the mouse model, Cdk4 R24C/R24C: Tyr- NRAS Q 61K. At early stages, such lesions are not detectable in the visible spectrum. With densities of many thousands of microscopic lesions per animal, 6mm diameter, full thickness skin biopsies are likely to contain stage 1 or 2 lesions.[70] Fresh biopsies were taken from supplied tissue. Figure 4 shows the experimental setup.

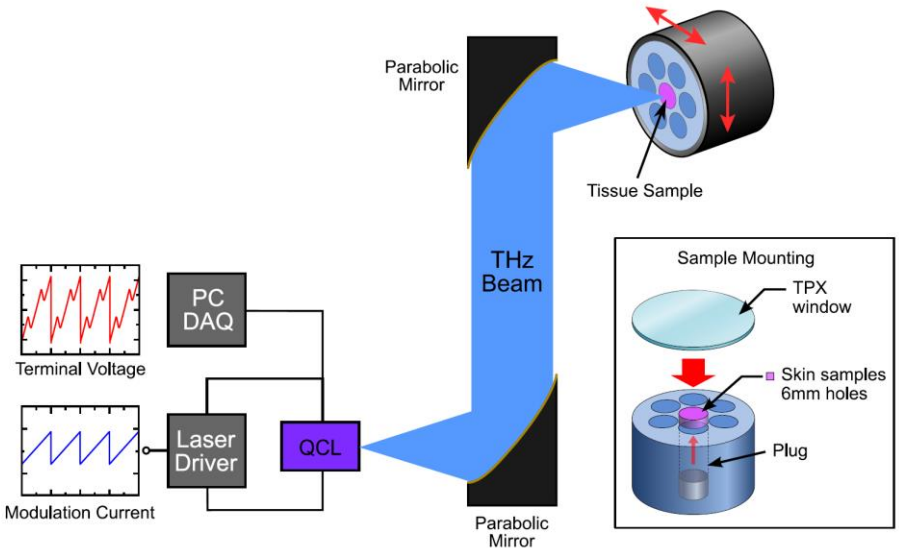

Figure 4. Schematic diagram of the setup used for tissue imaging experiment. The inset illustrates the exploded view of our tissue sample holder.

Using the experimental apparatus described above, we performed tissue imaging of a fresh punch biopsy over a seven hour period from excision. Biopsy specimen was maintained in normal saline prior to, and during the scan procedure in a purpose built specimen holder and window. The first scan was performed at one hour post excision. In this experiment, a two-dimensional array of time-domain waveforms was acquired, with one waveform associated with each pixel in the image. Experimentally-acquired signals were treated as described in Ref. [9].

Biopsy tissue was fixed in 10% formalin solution immediately following scanning. Tissue was blocked, sectioned *en face* using 10 μm slice thickness. SOX10 stain[71] was used as a melanocyte specific indicator to delineate the regions of the specimen with melanocyte involvement.

Three straightforward reductions were performed to derive a color-mapped image of the melanoma model specimen, and are shown in Fig. 5. The first reduction, shown in C1, depicts the RMS value of the SM signal, and the second reduction, shown in C2, depicts the peak power in the FFT spectrum associated with the SM signal. Both of these reductions contain amplitude- like information. The third reduction, shown in C3, depicts the mean cross-correlation that each pixel has with its cardinal neighbors. Each reduction is presented for a series of seven hourly THz scans.

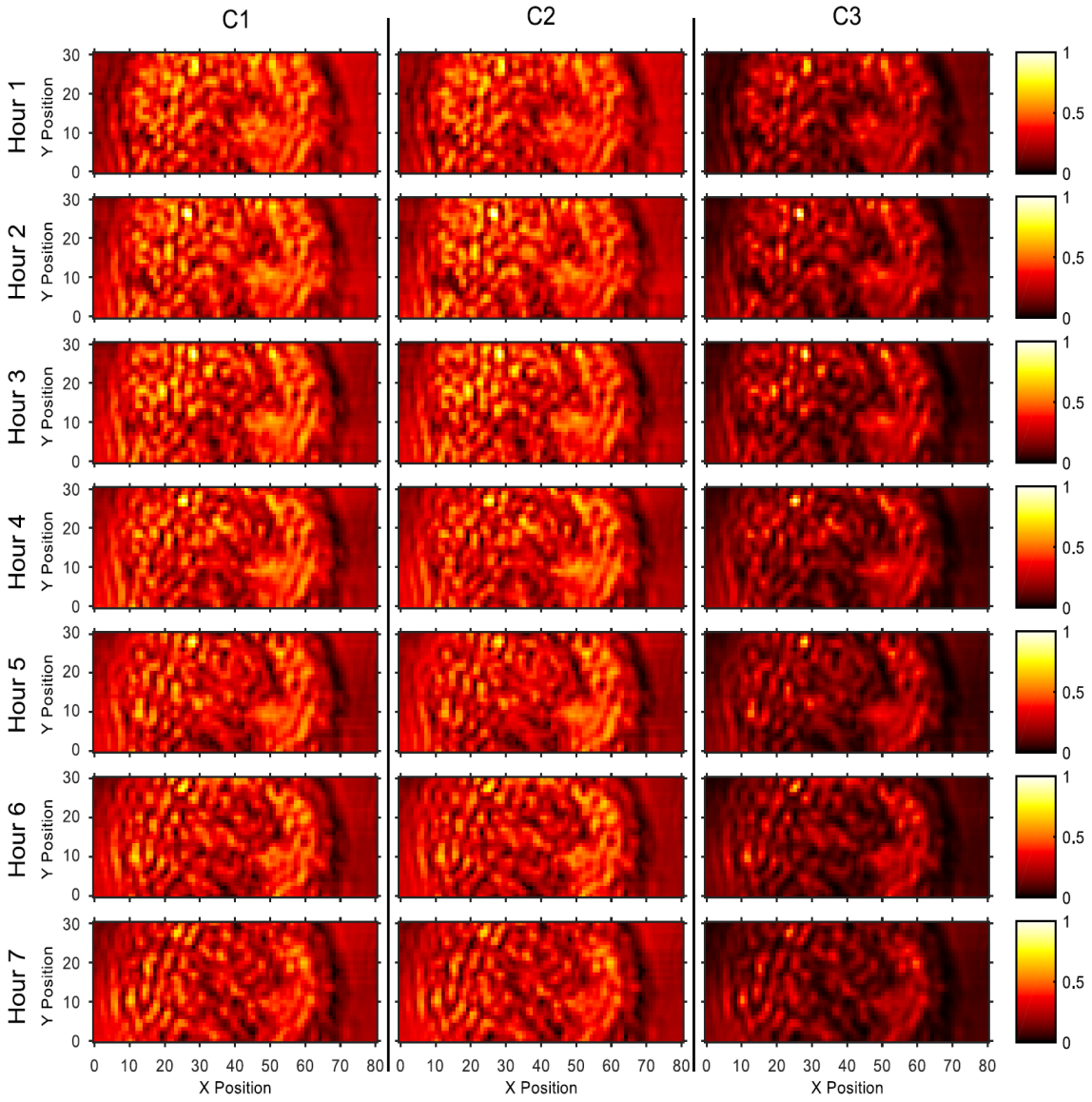

Figure 5. Three sets of THz images where each row represents a scan performed at hourly intervals. C1: RMS. C2:FFT Peak Power. C3: Spatial Cross-correlation.

Figure 6 (a) shows a photograph the murine tissue sample, (b) shows an *en face* section of SOX10 stained histology, and (c) depicts the cross-correlation that each pixel has with itself over the series of seven hourly THz scans.

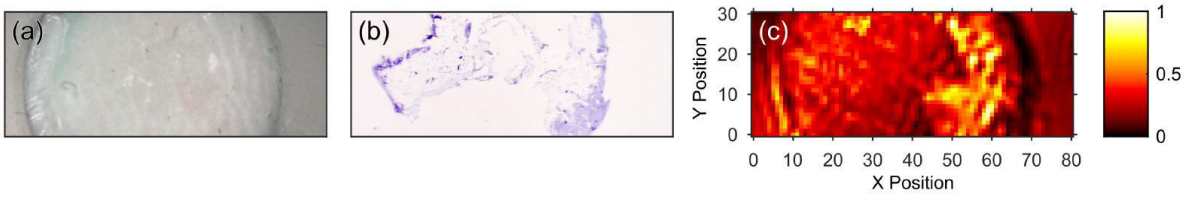

Figure 6. (a) Photograph the murine tissue sample, (b) An *en face* section of SOX10 stained histology, and (c) Cross-correlation that each pixel has with itself over the series of seven hourly THz scans.

6. CONCLUSION

Pulsed THz LFI techniques are a promising pathway to higher-temperature THz QCL imaging, long-range screening, and materials identification. In this work we demonstrated in simulation the pulsed operation of THz QCLs, using models for single-mode single-cavity and multi-mode coupled-cavity THz QCLs experiencing optical feedback. Moreover, we highlighted the potential of LFI at THz frequencies in biological applications, by presenting an LFI experiment with a THz QCL operating in cw, which images malignant melanoma precursor lesions in the transgenic mouse model. It remains a significant technological challenge to realize pulsed LFI systems in the laboratory.

ACKNOWLEDGMENTS

This research was supported by the Australian Research Council's Discovery Projects funding scheme (DP 160 103910), the Queensland Government's Advance Queensland programme, and the European Cooperation in Science and Technology (COST) Action BM1205. We also acknowledge support of the EPSRC UK (Grants EP/J017671/1 and DTG award) and the Royal Society (Wolfson Research Merit Awards WM110032 and WM150029).

REFERENCES

[1] Köhler, R., Tredicucci, A., Beltram, F., Beere, H. E., Linfield, E. H., Davies, A. G., Ritchie, D. A., Iotti, R. C., and Rossi, F., "Terahertz semiconductor-heterostructure laser," Nature 417(6885), 156–159 (2002).

[2] Barbieri, S., Alton, J., Beere, H. E., Fowler, J., Linfield, E. H., and Ritchie, D. A., "2.9 THz quantum cascade lasers operating up to 70 K in continuous wave," Appl. Phys. Lett. 85(10), 1674–1676 (2004).

[3] Luo, H., Laframboise, S. R., Wasilewski, Z. R., Aers, G. C., Liu, H. C., and Cao, J. C., "Terahertz quantum-cascade lasers based on a three-well active module," Appl. Phys. Lett. 90(4), 041112 (2007).

[4] Belkin, M. A., Fan, J. A., Hormoz, S., Capasso, F., Khanna, S. P., Lachab, M., Davies, A. G., and Linfield, E. H., "Terahertz quantum cascade lasers with copper metal-metal waveguides operating up to 178 K," Opt. Express 16(5), 3242–3248 (2008).

[5] Green, R. P., Xu, J. H., Mahler, L., Tredicucci, A., Beltram, F., Giuliani, G., Beere, H. E., and Ritchie, D. A., "Linewidth enhancement factor of terahertz quantum cascade lasers," Appl. Phys. Lett. 92(7), 071106 (2008).

[6] Khanna, S. P., Chakraborty, S., Lachab, M., Hinchcliffe, N. M., Linfield, E. H., and Davies, A. G., "The growth and measurement of terahertz quantum cascade lasers," Physica E: Low Dimens. Syst. Nanostruct. 40(6), 1859–1861 (2008).

[7] Ravaro, M., Barbieri, S., Santarelli, G., Jagtap, V., Manquest, C., Sirtori, C., Khanna, S. P., and Linfield, E. H., "Measurement of the intrinsic linewidth of terahertz quantum cascade lasers using a near-infrared frequency comb," Opt. Express 20(23), 25654–25661 (2012).

[8] Vitiello, M. S., Consolino, L., Bartalini, S., Taschin, A., Tredicucci, A., Inguscio, M., and De Natale, P., "Quantum-limited frequency fluctuations in a terahertz laser," Nature Photon. 6(8), 525–528 (2012).

[9] Rakić, A. D., Taimre, T., Bertling, K., Lim, Y. L., Dean, P., Indjin, D., Ikonić, Z., Harrison, P., Valavanis, A., Khanna, S.P., Lachab, M., Wilson, S. J., Linfield, E. H., and Davies, A. G., "Swept-frequency feedback interferometry using terahertz frequency QCLs: a method for imaging and materials analysis," Opt. Express 21(19), 22194–22205 (2013).

[10] Ravaro, M., Jagtap, V., Santarelli, G., Sirtori, C., Li, L. H., Khanna, S. P., Linfield, E. H., and Barbieri, S., "Continuous-wave coherent imaging with terahertz quantum cascade lasers using electro-optic harmonic sampling," Appl. Phys. Lett. 102(9), 091107 (2013).

[11] Dean, P., Valavanis, A., Keeley, J., Bertling, K., Lim, Y. L., Alhathlool, R., Burnett, A. D., Li, L. H., Khanna, S. P., Indjin, D., Taimre, T., Rakić, A. D., Linfield, E. H., and Davies, A. G., "Terahertz imaging using quantum cascade lasers — a review of systems and applications," Journal of Physics D: Applied Physics 47(37), 374008 (2014).

[12] Taimre, T., Nikolić, M., Bertling, K., Lim, Y. L., Bosch, T., and Rakić, A. D., "Laser feedback interferometry: a tutorial on the self-mixing effect for coherent sensing," Adv. Opt. Photon. 7, 570–631 (2015).

[13] Dean, P., Lim, Y. L., Valavanis, A., Kliese, R., Nikolić, M., Khanna, S. P., Lachab, M., Indjin, D., Ikonić, Z., Harrison, P., Rakić, A. D., Linfield, E. H., and Davies, A. G., "Terahertz imaging through self-mixing in a quantum cascade laser," Opt. Lett. 36(13), 2587–2589 (2011).

[14] Lim, Y. L., Dean, P., Nikolić, M., Kliese, R., Khanna, S. P., Lachab, M., Valavanis, A., Indjin, D., Ikoni´c, Z., Harrison, P., Linfield, E. H., Davies, A. G., Wilson, S. J., and Rakić, A. D., "Demonstration of a self-mixing displacement sensor based on terahertz quantum cascade lasers," Appl. Phys. Lett. 99(8), 081108 (2011).

[15] Dean, P., Valavanis, A., Keeley, J., Bertling, K., Leng Lim, Y., Alhathlool, R., Chowdhury, S., Taimre, T., Li, L. H., Indjin, D., Wilson, S. J., Rakić, A. D., Linfield, E. H., and Giles Davies, A., "Coherent three-dimensional terahertz imaging through self-mixing in a quantum cascade laser," Appl. Phys. Lett. 103(18), 181112 (2013).

[16] Han, S., Bertling, K., Dean, P., Keeley, J., Burnett, A. D., Lim, Y. L., Khanna, S. P., Valavanis, A., Linfield, E. H., Davies, A. G., Indjin, D., Taimre, T., and Rakić, A. D., "Laser feedback interferometry as a tool for analysis of granular materials at terahertz frequencies: Towards imaging and identification of plastic explosives," Sensors 16(3), 352 (2016).

[17] Woodward, R. M., Cole, B. E., Wallace, V. P., Pye, R. J., Arnone, D. D., Linfield, E. H., and Pepper, M., "Terahertz pulse imaging in reflection geometry of human skin cancer and skin tissue," Phys. Med. Biol. 47(21), 3853–3863 (2002).

[18] Kim, S. M., Hatami, F., Harris, J. S., Kurian, A. W., Ford, J., King, D., Scalari, G., Giovannini, M., Hoyler, N., Faist, J., and Harris, G., "Biomedical terahertz imaging with a quantum cascade laser," Appl. Phys. Lett. 88(15), 153903 (2006).

[19] Pickwell, E. and Wallace, V. P., "Biomedical applications of terahertz technology," J. Phys. D: Appl. Phys. 39(17), R301–R310 (2006).

[20] Wallace, V. P., Fitzgerald, A. J., Pickwell, E., Pye, R. J., Taday, P. F., Flanagan, N., and Ha, T., "Terahertz pulsed spectroscopy of human basal cell carcinoma," Appl. Spectrosc. 60(10), 1127–1133 (2006).

[21] Taylor, Z. D., Singh, R. S., Culjat, M. O., Suen, J. Y., Grundfest, W. S., Lee, H., and Brown, E. R., "Reflective terahertz imaging of porcine skin burns," Opt. Lett. 33(11), 1258–1260 (2008).

[22] Joseph, C. S., Patel, R., Neel, V. A., Giles, R. H., and Yaroslavsky, A. N., "Imaging of ex vivo nonmelanoma skin cancers in the optical and terahertz spectral regions," J. Biophotonics 7(5), 295–303 (2012).

[23] Smye, S. W., Chamberlain, J. M., Fitzgerald, A. J., and Berry, E., "The interaction between terahertz radiation and biological tissue," Phys. Med. Biol. 46(9), R101–R112 (2001).

[24] Fitzgerald, A. J., Berry, E., Zinov'ev, N. N., Homer-Vanniasinkam, S., Miles, R. E., Chamberlain, J. M., and Smith,

M.A., "Catalogue of human tissue optical properties at terahertz frequencies," J. Biol. Phys. 29(2–3), 123–128 (2003).

[25] Pickwell, E., Cole, B. E., Fitzgerald, A. J., Pepper, M., and Wallace, V. P., "In vivo study of human skin using pulsed terahertz radiation," Phys. Med. Biol. 49(9), 1595–1607 (2004).

[26] He, M., Azad, A. K., Ye, S., and Zhang, W., "Far-infrared signature of animal tissues characterized by terahertz time-domain spectroscopy," Opt. Commun. 259(1), 389–392 (2006).

[27] Xu, J., Plaxco, K. W., and Allen, S. J., "Absorption spectra of liquid water and aqueous buffers between 0.3 and 3.72 THz," J. Chem. Phys 124(3), 036101 (2006).

[28] Huang, S. Y., Wang, Y. X. J., Yeung, D. K. W., Ahuja, A. T., Zhang, Y.-T., and Pickwell-MacPherson, E., "Tissue characterization using terahertz pulsed imaging in reflection geometry," Phys. Med. Biol. 54(1), 149–160 (2009).

[29] Sun, Y., Fischer, B. M., and Pickwell-MacPherson, E., "Effects of formalin fixing on the terahertz properties of biological tissues," J. Biomed. Opt. 14(6), 064017 (2009).

[30] Bennett, D. B., Li, W., Taylor, Z. D., Grundfest, W. S., and Brown, E. R., "Stratified media model for terahertz reflectometry of the skin," IEEE Sens. J. 11(5), 1253–1262 (2011).

[31] Lim, Y. L., Taimre, T., Bertling, K., Dean, P., Indjin, D., Valavanis, A., Khanna, S. P., Lachab, M., Schaider, H., Prow, T.W., Soyer, H. P., Wilson, S. J., Linfield, E. H., Davies, A. G., and Rakić, A. D., "High-contrast coherent terahertz imaging of porcine tissue via swept-frequency feedback interferometry," Biomed. Opt. Express 5, 3981–3989 (2014).

[32] Rakić, A. D., Taimre, T., Bertling, K., Lim, Y. L., Wilson, S. J., Nikolić, M., Valavanis, A., Indjin, D., Linfield, E. H., Davies, A. G., Ferguson, B., Walker, G., Schaider, H., and Soyer, H. P., "THz QCL self-mixing interferometry for biomedical applications," Proc. SPIE Terahertz Emitters Receivers and Applications V 9199, 91990M (2014).

[33] Li, L., Chen, L., Zhu, J., Freeman, J., Dean, P., Valavanis, A., Davies, A. G., and Linfield, E. H., "Terahertz quantum cascade lasers with >1 W output powers," Electron. Lett. 50(4), 309–311 (2014).

[34] Fathololoumi, S., Dupont, E., Chan, C., Wasilewski, Z., Laframboise, S., Ban, D., Mátyás, A., Jirauschek, C., Hu, Q., and Liu, H. C., "Terahertz quantum cascade lasers operating up to ∼ 200 k with optimized oscillator strength and improved injection tunneling," Opt. Express 20, 3866–3876 (2012).

[35] Rakić, A. D., Agnew, G., Qi, X., Taimre, T., Lim, Y. L., Bertling, K., Han, S., Wilson, S. J., Grier, A., Kundu, I., Li, L., Valavanis, A., Dean, P., Ikonić, Z., Cooper, J., Khanna, S. P., Lachab, M., Linfield, E. H., Davies, A. G., Harrison, P., and Indjin, D., "Terahertz frequency quantum cascade lasers: Optical feedback effects and applications," in [2016 International Conference on Numerical Simulation of Optoelectronic Devices (NUSOD)], 203–204 (July 2016).

[36] Agnew, G., Grier, A., Taimre, T., Lim, Y. L., Nikolić, M., Valavanis, A., Cooper, J., Dean, P., Khanna, S. P., Lachab, M., Linfield, E. H., Davies, A. G., Harrison, P., Ikonić, Z., Indjin, D., and Rakić, A. D., "Efficient prediction of terahertz quantum cascade laser dynamics from steady-state simulations," Appl. Phys. Lett. 106(16), 161105 (2015).

[37] Agnew, G., Grier, A., Taimre, T., Lim, Y. L., Bertling, K., Ikonić, Z., Valavanis, A., Dean, P., Cooper, J., Khanna, S. P., Lachab, M., Linfield, E. H., Davies, A. G., Harrison, P., Indjin, D., and Rakić, A. D., "Model for a pulsed terahertz quantum cascade laser under optical feedback," Opt. Express 24(18), 20554–20570 (2016).

[38] Agnew, G., Grier, A., Taimre, T., Lim, Y. L., Bertling, K., Ikonić, Z., Valavanis, A., Dean, P., Cooper, J., Khanna, S., Lachab, M., Linfield, E., Davies, G., Harrison, P., Indjin, D., and Rakić, A. D., "Interferometry via thermal modulation in low duty cycle pulsed terahertz QCLs," in [Proceedings of International Quantum Cascade Lasers School and Workshop (IQCLSW), Cambridge, September 2016, pp 187], (2016).

[39] Qi, X., Kundu, I., Dean, P., Agnew, G., Taimre, T., Indjin, D., Li, L., Linfield, E. H., Davies, A. G., and Rakić, A. D., "Modelling of mode competition characteristics in coupled-cavity terahertz quantum cascade lasers using multi-mode reduced rate equations," in [Proceedings of International Quantum Cascade Lasers School and Workshop (IQCLSW), Cambridge, September 2016, pp 205], (2016).

[40] Hübers, H.-W., Pavlov, S., Richter, H., Semenov, A., Mahler, L., Tredicucci, A., Beere, H., and Ritchie, D., "High-resolution gas phase spectroscopy with a distributed feedback terahertz quantum cascade laser," Appl. Phys. Lett. 89(6), 061115 (2006).

[41] Dean, P., Saat, N. K., Khanna, S. P., Salih, M., Burnett, A., Cunningham, J., Linfield, E. H., and Davies, A. G., "Dual-frequency imaging using an electrically tunable terahertz quantum cascade laser," Opt. Express 17(23), 20631–20641 (2009).

[42] Giehler, M., Kostial, H., Hey, R., and Grahn, H., "Suppression of longitudinal modes in two-sectioned, coupled-cavity GaAs/(Al, Ga) As terahertz quantum-cascade lasers," Appl. Phys. Lett. 91(16), 161102 (2007).

[43] Li, H., Manceau, J., Andronico, A., Jagtap, V., Sirtori, C., Li, L., Linfield, E., Davies, A., and Barbieri, S., "Coupled-cavity terahertz quantum cascade lasers for single mode operation," Appl. Phys. Lett. 104(24), 241102 (2014).

[44] Kundu, I., Dean, P., Valavanis, A., Chen, L., Li, L., Cunningham, J. E., Linfield, E. H., and Davies, A. G., "Discrete vernier tuning in terahertz quantum cascade lasers using coupled cavities," Opt. Express 22(13), 16595–16605 (2014).

[45] Donati, S., "Laser interferometry by induced modulation of cavity field," J. Appl. Phys. 49(2), 495–497 (1978).

[46] King, P. G. R. and Steward, G. J., "Metrology with an optical maser," New Scientist 17(323), 180 (1963).

[47] Churnside, J. H., "Laser Doppler velocimetry by modulating a CO2 laser with backscattered light," Appl. Opt. 23(1), 61–66 (1984).

[48] Nerin, P., Puget, P., Besesty, P., and Chartier, G., "Self-mixing using a dual-polarisation Nd:YAG microchip laser," Electron. Lett. 33(6), 491–492 (1997).

[49] Han, D., Wang, M., and Zhou, J., "Self-mixing speckle in an erbium-doped fiber ring laser and its application to velocity sensing," IEEE Photon. Technol. Lett. 19(18), 1398–1400 (2007).

[50] Dai, X., Wang, M., Zhao, Y., and Zhou, J., "Self-mixing interference in fiber ring laser and its application for vibration measurement," Opt. Express 17(19), 16543–16548 (2009).

[51] Lim, Y. L., Nikolić, M., Bertling, K., Kliese, R., and Rakić, A. D., "Self-mixing imaging sensor using a monolithic VCSEL array with parallel readout," Opt. Express 17(7), 5517–5525 (2009).

[52] Sudo, S., Ohtomo, T., Takahashi, Y., Oishi, T., and Otsuka, K., "Determination of velocity of self-mobile phytoplankton using a self-mixing thin-slice solid-state laser," Appl. Opt. 48(20), 4049–4055 (2009).

[53] Bertling, K., Lim, Y. L., Taimre, T., Indjin, D., Dean, P., Weih, R., Höfling, S., Kamp, M., von Edlinger, M., Koeth, J., and Rakić, A. D., "Demonstration of the self-mixing effect in interband cascade lasers," Appl. Phys. Lett. 103(23), 231107 (2013).

[54] Valavanis, A., Dean, P., Lim, Y. L., Alhathlool, R., Nikolić, M., Kliese, R., Khanna, S. P., Indjin, D., Wilson, S. J., Rakić, A. D., Linfield, E. H., and Davies, A. G., "Self-mixing interferometry with terahertz quantum cascade lasers," IEEE Sens. J. 13(1), 37–43 (2013).

[55] Donati, S., "Developing self-mixing interferometry for instrumentation and measurements," Laser Photon. Rev. 6(3), 393–417 (2012).

[56] Bosch, T., Bès, C., Scalise, L., and Plantier, G., "Optical feedback interferometry," in [Encyclopedia of Sensors], Grimes, C. A. and Dickey, E. C., eds., 1–20, American Scientific Publishers (2006).

[57] Giuliani, G., Norgia, M., Donati, S., and Bosch, T., "Laser diode self-mixing technique for sensing applications," J. Opt. A, Pure Appl. Opt. 4(6), S283–S294 (2002).

[58] Giuliani, G. and Donati, S., "Laser interferometry," in [Unlocking Dynamical Diversity: Optical Feedback Effects on Semiconductor Lasers], Kane, D. M. and Shore, K. A., eds., John Wiley & Sons, Chichester (2005).

[59] Scalari, G., Ajili, L., Faist, J., Beere, H., Linfield, E., Ritchie, D., and Davies, G., "Far-infrared ($\lambda \approx 87$ μm) bound-to-continuum quantum-cascade lasers operating up to 90 K," Appl. Phys. Lett. 82(19), 3165–3167 (2003).

[60] Indjin, D., Harrison, P., Kelsall, R. W., and Ikonić, Z., "Mechanisms of temperature performance degradation in terahertz quantum-cascade lasers," Appl. Phys. Lett. 82(9), 1347–1349 (2003).

[61] Paiella, R., Martini, R., Capasso, F., Gmachl, C., Hwang, H. Y., Sivco, D. L., Baillargeon, J. N., Cho, A. Y., Whittaker, E. A., and Liu, H. C., "High-frequency modulation without the relaxation oscillation resonance in quantum cascade lasers," Appl. Phys. Lett. 79(16), 2526–2528 (2001).

[62] Barbieri, S., Maineult, W., Dhillon, S. S., Sirtori, C., Alton, J., Breuil, N., Beere, H. E., and Ritchie, D. A., "13 GHz direct modulation of terahertz quantum cascade lasers," Appl. Phys. Lett. 91(14), 143510 (2007).

[63] Gellie, P., Barbieri, S., Lampin, J.-F., Filloux, P., Manquest, C., Sirtori, C., Sagnes, I., Khanna, S. P., Linfield, E. H., Davies, A. G., Beere, H., and Ritchie, D., "Injection-locking of terahertz quantum cascade lasers up to 35 GHz using RF amplitude modulation," Opt. Express 18(20), 20799–20816 (2010).

[64] Barbieri, S., Ravaro, M., Gellie, P., Santarelli, G., Manquest, C., Sirtori, C., Khanna, S. P., Linfield, E. H., and Davies, A. G., "Coherent sampling of active mode-locked terahertz quantum cascade lasers and frequency synthesis," Nature Photon. 5(5), 306–313 (2011).

[65] Grier, A., Dean, P., Valavanis, A., Keeley, J., Kundu, I., Cooper, J., Agnew, G., Taimre, T., Lim, Y. L., Bertling, K., Rakić, A. D., Li, L., Harrison, P., Linfield, E. H., Ikonić, Z., Davies, A. G., and Indjin, D., "Origin of terminal voltage variations due to self-mixing in terahertz frequency quantum cascade lasers," Opt. Express 24(19), 21948–21956 (2016).

[66] Acket, G. A., Lenstra, D., den Boef, A. J., and Verbeek, B. H., "The influence of feedback intensity on longitudinal mode properties and optical noise in index-guided semiconductor lasers," IEEE J. Quantum Electron. 20(10), 1163–1169 (1984).

[67] Taimre, T. and Rakić, A. D., "On the nature of Acket's characteristic parameter C in semiconductor lasers," Appl. Opt. 53(5), 1001–1006 (2014).

[68] Hamadou, A., Lamari, S., and Thobel, J.-L., "Dynamic modeling of a midinfrared quantum cascade laser," J. Appl. Phys. 105 (9), 093116 (2009).

[69] Petitjean, Y., Destic, F., Mollier, J. C., and Sirtori, C., "Dynamic modeling of terahertz quantum cascade lasers," IEEE J. Sel. Topics Quantum Electron. 17, 22–29 (2011).

[70] Wurm, Elisabeth M.T., Lin, Lynlee L., Ferguson, Blake, Lambie, Duncan, Prow, Tarl W., Walker, Graeme J. and Soyer, H. Peter, "A blueprint for staging of murine melanocytic lesions based on the Cdk4 R24C/R24C :: Tyr- NRAS Q 61K model," Exp. Dermatol., **21(**9), 676-681 (2012).

[71] Mohamed A, Gonzalez RS, Lawson D, Wang J, Cohen C., "SOX10 expression in malignant melanoma, carcinoma, and normal tissues," Appl. Immunohistochem. Mol. Morphol. **21**(6), 506-10 (2013).